Self-correcting Algorithm for Estimated Time of Arrival of Emergency Responders

Rreze Halili, F. Zarrar Yousaf, Nina Slamnik-Krijestorac, Girma M. Yilma, Marco Liebsch, Rafael Berkvens, Maarten Weyn

***Abstract*—Edge computing is one of the key features of the 5G technology-scape that is realizing new and enhanced automotive use cases for improving road safety and emergency response management. Back Situation Awareness (BSA) is such a use case that provides advance notification to the vehicles of an arriving emergency vehicle (EmV). This paper presents an algorithm for enhancing the accuracy of the advance Estimated Time of Arrival (ETA) notification of an approaching emergency vehicle EmV towards vehicles, ensuring timely reaction by the vehicles to create a clear corridor for the EmV to pass through unhindered, thereby saving precious time to reach the emergency event in a safe manner. Features of the presented solution are: I. the algorithm self-correction approach, II. adaptive or dynamic dissemination area size allocation in reaction to traffic changes, and III. evaluation of the ETA accuracy. Based on real travel time data measurements, the performance of the algorithm has been evaluated and compared using Kalman filter, Filter-less method, Moving Average, and Exponential Moving Average filters. It is observed that the Kalman filter provides better accuracy on the ETA estimation, by reducing the estimation error by around 14% on average.**

***Index Terms*—5G, C-ITS, C-V2X, ETA, MEC.**

I. Introduction

The latest advances in 5G technology enablers are leveraged by vehicular networks in ways not perceivable before. These advances are expected to improve public safety in terms of avoidance of traffic accidents and improvement of emergency response time, considered as a lifesaving factor.

There is a significant research conducted to find a meaningful relationship between the emergency response time and the probability of fatal outcomes, and the results prove that reduction of the overall response time plays a critical role in emergency situations [1–4]. For example, in [2] a 10 min reduction in the emergency response time decreases the probability of death by one-third. The regulatory requirements of some developed countries call for less than 10 minutes reaction time to life-threatening incidents, which becomes difficult to achieve especially during heavy traffic conditions.

Today the drivers get informed of the presence of an approaching Emergency Vehicle (EmV), which can be an ambulance, a police vehicle, or a fire brigade, through blaring sirens and flashing lights. Since the drivers get alerted only when the EmVs are within audio/visual range, they have limited time and space to react and manoeuvre away from the path of the EmV in a timely, calm, coordinated, and safe manner. Creating a clear corridor for the EmV becomes more difficult and time consuming when there is high traffic density. This situation not only causes delays in emergency services response time but can also cause accidents. According to a report published by National Highway Traffic Safety Administration (NHTSA) office of Emergency Medical System (EMS), 70% of all ambulance crashes occur while operating in an emergency mode [5]. According to another report, [6], 66% of firetruck crashes occur when the truck is being used during an emergency.

To address these challenges a lot of research work has been done on modelling and optimizing the ambulance response time. As will be described in the Section II, most of the solutions propose methods calling for route optimization that enables the circumvention or avoidance of congested locations in order to ensure the timely arrival of the EmV to the intended destination. However, such solutions are limited depending on the countries considered, time of the day/year, weather, traffic conditions and limited route options.

Given the above stated limitations we present a more universal V2X method that leverages the multi-access edge computing (MEC) system, which is an integral part of 5G mobile network infrastructure [7], together with the Network Function Virtualization (NFV), and Software Defined Networking (SDN) as key technology enablers [8]. The reason for proposing a vehicle-to-network (V2N) solution is because the vehicle-to-vehicle (V2V) communication range is limited, for example up to 300 meters for PC5 links, for providing enough time for the drivers to calmly inter-coordinate between themselves and/or free the lane to create a safety corridor for the fast approaching EmV. Our proposed Back-Situation Awareness (BSA) method enables an early notification of the ETA of an approaching EmV while it is out of the audio visual range of the vehicles along its route-path. As seen in Fig. 1, the BSA service is instantiated within the MEC system predicting the ETA values with reference to different way-points along the selected route-path of the EmV. These values known as ETA-1, ETA-2, ETA-3, and ETA-4 are disseminated to the vehicles in the dissemination areas between two consecutive way-points referenced as WP-1, WP-2, WP-3, and WP-4, respectively Dissemination Area 1, Dissemination Area 2, Dissemination Area 3, and Dissemination Area 4.

This work extends our previous work [9] where a basic version of the BSA algorithm was implemented using Kalman filter [10] and analysed on fixed dissemination areas. The analysis showed that the accuracy of the ETA value prediction is intrinsically linked to the dissemination area size and the traffic density in each dissemination area. The challenge therefore was to develop a BSA algorithm that is able to self-

Manuscript received September, XX, 2021; revised XXX, XX, 2021.

R. Halili, N. Slamnik-Krijestorac, R. Berkvens, M. Weyn, are with the University of Antwerp - imec, IDLab, Antwerp, Belgium, and F. Zarrar Yousaf, G. M. Yilma, M. Liebsch, are with the NEC Laboratories Europe GmbH, Germany, (e-mail: rreze.halili@uantwerpen.be, zarrar.yousaf@neclab.eu, nina.slamnikkrijestorac@uantwerpen.be, girma.yilma@neclab.eu, marco.liebsch@neclab.eu, rafael.berkvens@uantwerpen.be, maarten.weyn@uantwerpen.be)

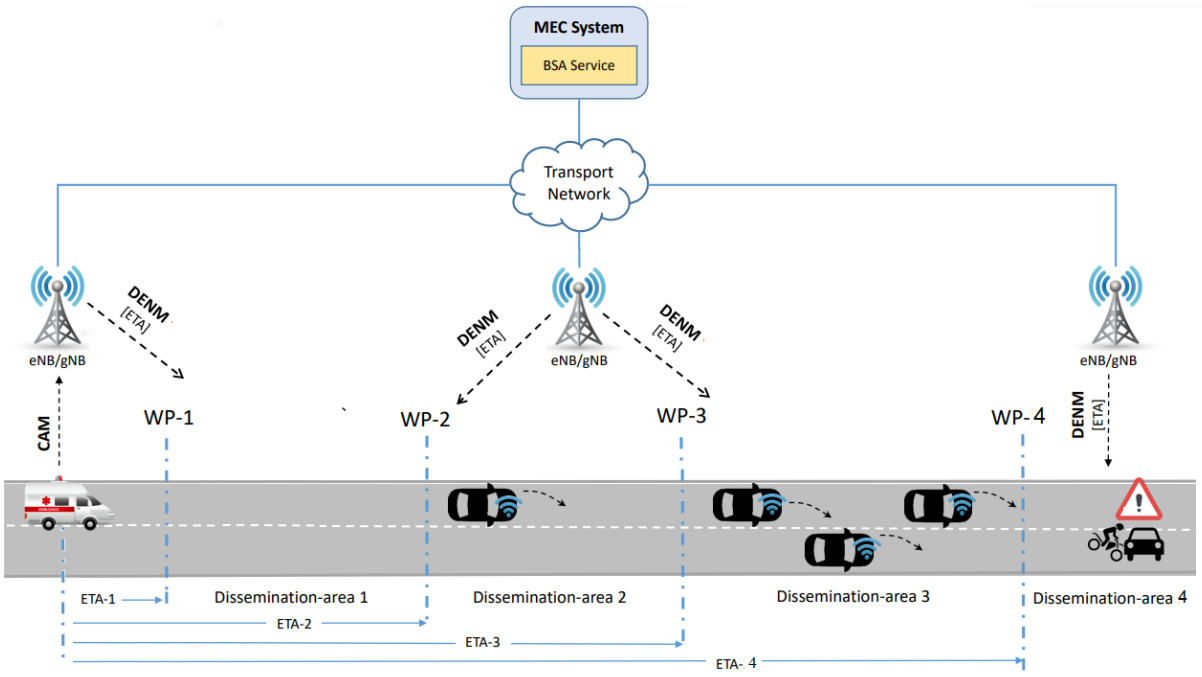

Fig. 1: Back Situation Awareness Overview.

correct dynamically itself taking into consideration the error-size and the traffic density to predict accurate ETA values.

For this purpose the scope of research has been expanded beyond [9], thereby the extended new algorithm solution takes into account prevailing traffic conditions and estimation errors when determining the optimum size of the dissemination areas that will give an accurate prediction of the ETA. So, the algorithm is able to dynamically resize the dissemination areas size in order to enhance the prediction accuracy. Moreover, we perform a comparative analysis of different filtering methods to determine which one would give an accurate ETA values prediction. We also observe and discuss the impact of the frequency of the input data from the EmV on the prediction accuracy when deriving ETA values.

For our analysis, we compare our results with the experimental data measurements reflecting the actual time of arrival (ATA) that is measured and obtained on the Smart Highway testbed[1] placed on the E313 highway in Antwerp, Belgium.

The rest of the paper is organized as follows. Section II provides Related work, followed by Section III presenting the use case of the BSA scenario and providing a system's perspective. Section IV gives details about the dynamic self-correcting algorithm for accurate ETA prediction and related concepts together with the filtering techniques. The analysis and performance evaluation of the ETA algorithm within the BSA application in terms of accurate calculation and dynamic dissemination of the ETA is provided in Section V, followed by Section VI concluding the paper.

II. Related Work

Along with the growing needs for transportation, the ever-increasing number of vehicles causes numerous issues on the roads and highways such as traffic jams, car crashes, fatalities, etc. Thus, most of the research efforts on the situation awareness in vehicular scenarios tend to analyse methods that support the Emergency Management Systems to reduce patient mortality, to prevent disability, and to improve chances of recovery [11]. One of the key factors towards achieving these objectives is the emergency response time, which is considered as crucial for saving people's life. Thus, the relationship between the emergency response time and the survival rate has been part of different research works and some of them are presented in Table I and discussed as follows.

TABLE I: Overview of related work.

Research direction		Works
non-V2X concepts	evaluation of the EMS performance	[12–15]
	prediction of the EmV's travel time	[10,16–18]
V2X concepts	V2V	[19–27]
	V2I	[28]
	V2N	[29]

According to Nicholl et al. [12] a 10-km increase in straight-line distance is associated with around a 1% absolute increase in mortality, while Pell et al. [13] concluded that reducing ambulance response times to 5 minutes could almost double the survival rate for cardiac arrests not witnessed by ambulance crews.

Different predictive models, filters, routing, and navigation systems are used together with large historical datasets collected on different cities to optimize the route which the EmV should follow to avoid traffic, to have an accurate time of arrival estimation for the body expecting at the emergency units, and to have an efficient way of utilizing emergency services and resources. The proposed solutions depended on the countries considered and also on the time of the day, year, weather, and traffic condition.

[1]Smart Highway: https://www.fed4fire.eu/testbeds/smart-highway/

Iannoni et al. [14] provide an extension of the hypercube model, combined with the hybrid genetic algorithms, to optimize the configuration and operation of the emergency response time. The study provided by Iannoni et al. [14] suggests the relocation of the ambulance bases and their area of work, as a way to reduce i) the average user response time, ii) imbalance of the ambulances' workloads, and iii) the fraction of calls not serviced within a predetermined threshold. Poulton et al. [15] represents application of a data-driven methodology for route selection and the estimation of arrival times of ambulances travelling with blue lights and sirens on. This methodology recognizes only historical data collected internally by the emergency ambulance services, thereby not considering any real-time information, traffic, or related context information retrieved from the external systems (e.g., traffic management systems, cellular network services, etc.).

Regarding technology despite the disadvantage of the short-range emergency notifications, most of the research effort in enhancing situation awareness on the roads is focused on the Vehicle-to-Vehicle (V2V) technology, as it can be seen in the Table I. Among these works, an extensive effort has been conducted so far to reduce the delay of operation for emergency responders [19,20,28]. In their survey on urban traffic management system using wireless sensor networks [19], Nellore and Hancke recognize the schemes for prioritizing EmVs, as well as the congestion avoidance by decreasing the average waiting time for vehicles at the intersection, as a foundation for the future research. Tackling the intersection assistance systems, Joerer et al. [21] show that the current *state-of-the-art* congestion control mechanisms are not able to support intersection assistance adequately, due to the lack of fine-grained prioritization among vehicles. Since these existing congestion control mechanisms provide an equal share of communication opportunities to all vehicles, not considering the difference of road traffic situations or individual vehicles such as an EmV, the exchange of the traffic information cannot be done in a timely manner. Therefore, Joerer et al. [21] propose an improvement, which allows vehicles in critical situations at intersections to be temporarily exempted from congestion control, enabling them to communicate with possible collision candidates more frequently, through the so-called beaconing solutions that rely on one-hop broadcasting and 802.11p technology [21].

One of the interesting features on broadcasting awareness messages is the dissemination of Time of Arrival (ToA) of emergency vehicles. This way, the surrounding civilian cars can anticipate at which moment they should clear the lane. Senart et al. [23] study a reliable mechanism for transmitting information about EmV's ToA, using a wireless medium, and a feedback system. In their work [23], Senart et al. proposed a method to disseminate information on EmV's arrival and to provide real-time feedback to EmV in case the quality of the communication is degraded. In this kind of scenario, the EmV will be informed that certain vehicles may not have been warned, thus receiving a recommendation to slow down. Another approaches for disseminating information about EmV are presented by Kapileswar et al. [24], Johnson [25], Metzner and Wickramarathne [27], and Hadiwardoyo et al. [26], where they study relying on V2V connection to disseminate information on the location and the route path of emergency vehicles in real time, in order to provide vehicles in a closer proximity with an ample time to make driving decisions by considering incoming alerts.

Nevertheless, as already mentioned a drawback of the V2V communication is its short range, which is not sufficient for the drivers to timely react and clear the lane for the approaching EmV. Thus, an attempt to utilize V2I communication for that purpose is presented by Moroi and Takami [28]. To significantly decrease travel time for EmVs, Moroi and Takami [28] proposed utilizing the Roadside Units (RSUs) that support EmVs by notifying other vehicles about the EmV's route.

The network infrastructure and vehicle need to react with the latency below 100ms [29] to achieve higher safety levels by being less dependent on the driver's actions. This of course requires service availability in the edges close to the vehicles. Due to a still limited range that they cover, most of the operational requirements for vehicular applications cannot be fulfilled by RSUs [30]. On the other hand, cellular technologies successfully cope with this challenge since base stations usually cover larger regions than short range gateways (e.g., RSUs) [31]. Therefore, 5G systems and Multi-Access Edge Computing (MEC) are expected to improve the current support for V2X use cases [30,32], with the opportunity to significantly extend the notification range, and to decrease the delay by deploying vehicular applications at the network edge. By utilizing the cellular infrastructure, the management and orchestration entities, network controllers, and application services, are all fed with global information that helps them to notify civilian vehicles about emergency situations in extended regions, unlike in the case of short range communications where the local information in each vehicle does not include a broad view of the overall network.

It is in view of the above observations and shortcomings that we propose the BSA service the details of which are described in the subsequent sections.

III. Back Situation Awareness (BSA) Solution

A. BSA Use Case

As indicated above, the main objective of the BSA service is to improve the emergency response time, which is achieved by the early notification/dissemination of the EmV's ETA to the vehicles, allowing them enough time to create a clear corridor for the EmV to pass through unhindered.

There are different definitions of the emergency response time. A general overview found in many standards defines the emergency response time as the overall time being comprised of four unique time intervals, which include the activation, response or preparation, on scene, and transport intervals [33,34].

As shown in Fig. 2 when the Emergency center is notified about an emergency event we consider this as the activation time. Then the time which is required to have EmV dispatched to the emergency case is known as the preparation time. The time spend on the way to reach the destination is the travel time. The time spent on the event is the on-scene interval, and finally, the time spent from ambulance departure to the hospital is the travel time. In each emergency response time interval the developed BSA application within the MEC has its role, and uses its components and operations to initiate the algorithm, to calculate the ETA, to disseminate it on the

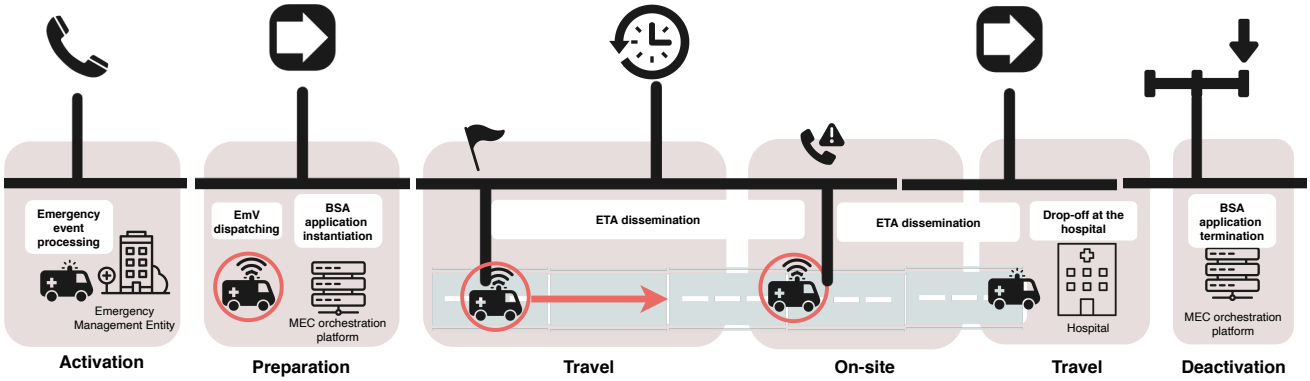

Fig. 2: Emergency response process with respective operations.

upcoming route-path, and at the end to terminate the use of the ETA algorithm (see Fig. 2).

A high-level overview of the BSA use case is illustrated in Fig. 1, which shows an EmV on route towards the event location. The event information is first received by an Emergency Management Entity (EME), such as 112 or 911 Headquarter (HQ), which dispatches an EmV providing it with the event location addresses (referred to as destination address), the route-path to follow, and the IP address of the BSA service. While heading towards the destination it will periodically start sending the ETSI Cooperative Intelligent Transport System (C-ITS) Cooperative Awareness Message (CAM) notifications [35] via the mobile network infrastructure towards the BSA service instance, which is instantiated on a MEC system as a MEC application [36].

The BSA service is able to parse the information encoded in the received CAM notifications such as speed, location, direction of the EmV. Based on these parameters, the BSA service application derives the value of ETA from the EmV's current location with reference to the respective way-points (Way-Points (WPs)) specified by the BSA service application along the designated route-path of the EmV up until the EmV's destination. Note that the destination of the EmV corresponds to either the event location and/or the final destination such as a hospital in case the EmV is an ambulance. BSA service application calculates ETA values ETA-1, ETA-2, ETA-3, and ETA-4 with reference to WP-1, WP-2, WP-3, and WP-4 respectively. The derived ETA values are then encoded in the ETSI ITS Decentralized Environmental Notification Message (Decentralized Environment Notification Message (DENM)) [37], which is then geo-casted in the respective dissemination areas. It should be noted that the dissemination area is the area between two successive WPs, and its size depends on the input parameters. Thus the ETA-1, ETA-2, ETA-3, and ETA-4 will be broadcasted in Dissemination Area 1, Dissemination Area 2, Dissemination Area 3, and Dissemination Area 4 respectively (see Fig. 1) . All the vehicles that are on the route-path of the EmV will process the received DENM notifications to extract the ETA values to be displayed on the vehicle's control panel. This will give the drivers an estimate of when to expect the EmV to arrive and thus manoeuvre to create a clear corridor for the EmV to pass through un-hindered in a safe manner.

B. BSA Service Application Design

Fig. 1 gives the design overview of the BSA service application, which is envisaged to run as a Virtual Application Function (VAF) deployed and instantiated on the MEC system. Fig. 3 shows the functional elements that are chained to deliver the BSA service. Fig. 3 also depicts the required interfaces enabling the BSA application to connect with the external entities. Interfaces A, B, and C are designed in a respective order to: i) receive upstream CAMs originating from the EmV with a specified frequency in Hz, ii) dispatch a DENM containing the derived ETA value for a specific dissemination area, and iii) maintain connectivity with a peering BSA application instance that may be running in another edge domain belonging to a different operator.

The EmV, after receiving the IP address of the MEC host where the BSA service is instantiated from the EME, will start to transmit the CAMs periodically towards the BSA service on the MEC host. These messages will be received on interface A, to be processed by the ITS protocol stack. In our case, this stack is provided by Vanetza, an open-source implementation of the ETSI C-ITS protocol suite [38]. The receive function of the Vanetza protocol suite will extract the CAM notification from the received IP packet. The decoding function, which is a simple helper function supporting Vanetza, will parse, extract and filter the information relevant for the BSA algorithm from the CAM notification, and prepare an input data for the BSA algorithm. The input parameters to the BSA are: i) the identification of EmV (EmV ID), ii) the speed of the EmV, iii) the current location of the EmV, iv) its destination, and v) direction of the EmV.

The BSA algorithm, marked in red in Fig. 3, is at the heart of the BSA service and the main contribution of this paper. It will calculate the ETA values for the respective dissemination area(s) each time it receives the CAM notification and evaluate the estimation error, based on which it will take corrective actions for error minimization by readjusting the size of the dissemination areas. The details of the BSA algorithm are presented in Section IV while its performance analysis can be found in the Section V-B.

Along with the ETA calculation operations, the BSA algorithm is storing the state of the application that refers to the information on the vehicle's speed, location, and destination, in the state database (State DB in Fig. 4). The state database plays a significant role in the communication between two

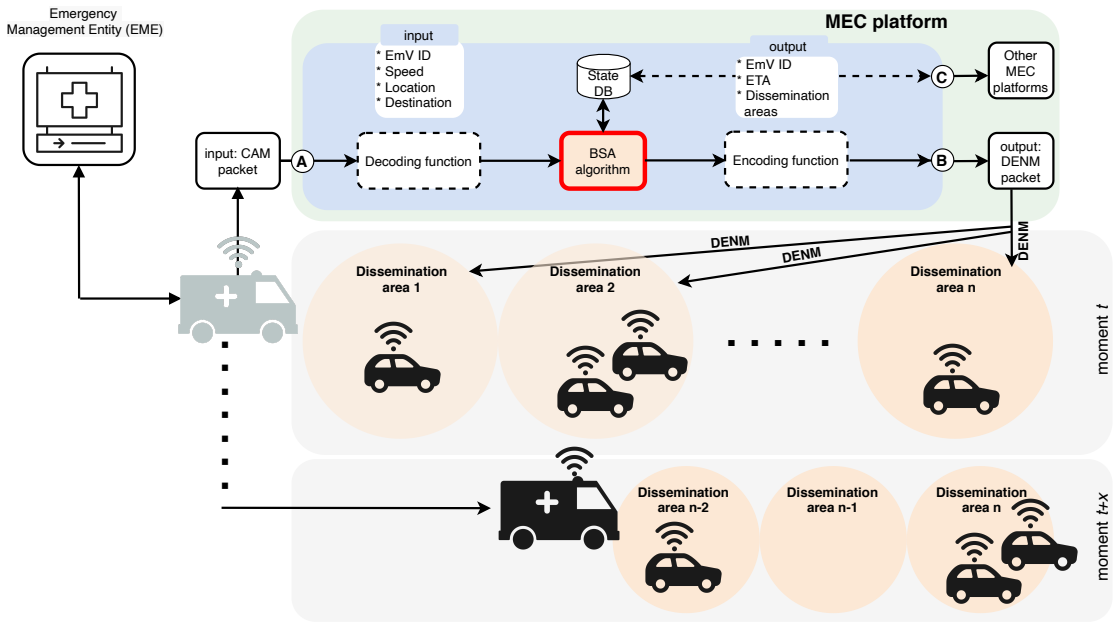

Fig. 3: BSA operation overview.

peering BSA service application instances running in two edge domains, thereby allowing the sharing of the EmV-specific meta information from one edge domain to the other via interface C (Fig. 3). This not only extends the range of the BSA service, but is also done in case the mobile network infrastructure along the route-path may belong to more than one operator with different MEC systems. However, the coverage of multi-operator domains is out of the scope of this paper.

Furthermore, the output of the BSA algorithm, i.e., mainly the ETA values for respective dissemination areas, is being processed by another helper function of the ITS protocol stack, referred to as Encoding Function in Fig. 3. This function has the task to prepare ETA notifications for the different dissemination areas by passing the information on: i) EmV ID, ii) calculated ETA value, and iii) dissemination area, to the transmit function of the Vanetza ITS protocol stack. The ITS protocol stack will encode this information in the ETSI ITS DENM a notification message, and dispatch it towards the mobile network infrastructure via interface B. This DENM notification is then disseminated (e.g., via broadcast) in the respective Dissemination Areas.

Each of the functional components comprising the BSA service is implemented as a visualized MEC service or MEC application, and thus instantiated on a MEC system. Fig. 4 gives the overview of the BSA service in the context of the standard ETSI MEC system architecture [36], and functional scope of each component is summarized below:

1) **BSA Application:** - This is proposed to be deployed as a *MEC application* [36] where the logic of assigning WPs on the route-path and computing ETA values with reference to these WPs is located. Additionally, this can also deduce maneuver recommendations to the vehicles being notified. This corresponds to the BSA Algorithm functional entity in Fig. 4.
2) **C-ITS Protocol Service:** This is proposed to be a *MEC service* [36] for decoding/parsing received C-ITS awareness and notification messages (CAM/DENM) for information relevant to the BSA application instance and for encoding ETA values in the DENM for notifying the vehicles. This corresponds to the ITS protocol stack and the decoding/encoding helper function entities in Fig. 4.
3) **Map Service:** This is proposed to be a MEC service that can be consumed by the BSA application for getting geospatial information, such as route-path information/plan based on which it can specify WPs along the route-path, and also get more information on the type of road the EmV is traveling on.
4) **State DB:** This is proposed to be the database where the meta-data/state-information of the EmV decoded/parsed by the C-ITS protocol service from the periodically received CAMs/DENMs are stored, which are then consumed by the BSA application for calculating ETA values, and optionally maneuver recommendations. This corresponds to the State DB entity in Fig. 4.
5) **Dissemination Service:** This service is used to disseminate the EmV's ETA information to the vehicles in front of the EmV. The distribuation of the ETA values in done within the relevant dissemination areas. As explained above a dissemination area is known as a region between two successive WPs.The BSA application encodes the ETA vector in a Cooperative Intelligent Transport System (C-ITS) DENM [37], and broadcasts it in a geo-casted dissemination area. The respective ETA value will be displayed on the control panel if the vehicles which in front of the EmV while heading to the emergency case.

The other functional elements shown in Fig. 4 are specified in the ETSI GS MEC 003 v2.1.1 standard [36] and are used for the management and orchestration of the BSA related MEC applications and MEC services as defined above. It should be noted that the EME is able to access the BSA system via the Customer Facing Service (CFS) interface. The details of the design of the BSA service components along with the details

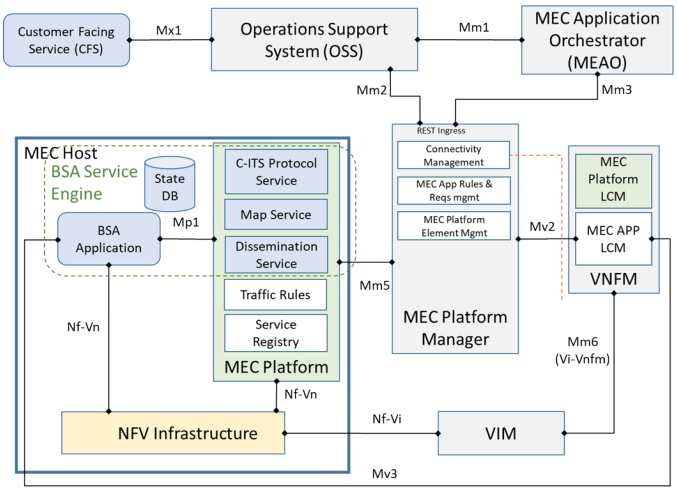

Fig. 4: BSA Service in the context of MEC system.

of the service orchestration and life-cycle management has already been described in our previous work [9].

IV. Estimated Time of Arrival Algorithm

A. ETA algorithm workflow

As described above, the BSA Algorithm takes as inputs the location, speed, ID, and destination (i.e., the location of emergency event) of the EmV for the calculation of the Estimated Time of Arrival (ETA) values with reference to the multiple WPs along the EmV's route path (see Fig. 3).

The workflow of the algorithm is shown in Algorithm 1. The MEC system will continuously listen to potential input information. In the case of the first received CAM it will be decoded and delivered to the BSA application. Then the system will collect and analyze the input data. The first step is to define the current geo-location of the reference object which in our case is an emergency vehicle. Then, the algorithm checks the required destination and uses Map Service to determine the route-path that EmV should follow headed to this destination. Considering the route path defined by the way-points, the algorithm will derive the ETAs for all dissemination areas, and create an ETA vector that will be broadcasted to the vehicles in front of the EmV using DENM and 5G mobile network infrastructure.

Depending on the frequency of input CAMs, which can be 1Hz, 2Hz, or 10Hz, the algorithm will have the input information again. With the upcoming CAM notification, the algorithm will have to check the position of the EmV and the time stamp at which this position was recorded. We consider this value as the Actual Time of Arrival (ATA), and is further used to check the accuracy of the previously recorded and transmitted ETA. This error value which displays the difference between ATA and ETA is considered as performance indicator and is used as feedback correction index for the following calculation of the ETA. Then depending on the ATA value and actual speed of the EmV, the algorithm determines the size of the dissemination areas and the number of reference WPs. The so called estimation error can result in a different sign. It will be positive if the ATA $>$ ETA and vice versa.

This algorithm will continue this trend until the EmV arrives at the destination. On such case the application terminates.

Algorithm 1: Workflow of the traffic signal for the main algorithm.

Result: Estimated Time of Arrival (ETA)
Start;
ϵ = 0sec ; step 1; **while** *EMV Not arrived at Destination* **do**
  Listen to arrival of CAM Notification;
  Get current geo-location of EmV;
  if *EmV moved from previous position* **then**
    Determine the Actual time of Arrival (ATA);
    $ETA - ATA = \zeta$;
    if $\zeta \neq \epsilon$ **then**
      Go to step x;
    else
      Re-evaluate the number and size of dissemination areas and ETA values per dissemination areas; $ETA_P = ATA$;
      Derive/Adjust coordinates for each dissemination area;
      Go to step 1;
    end
  else
    Derive the ETA for all dissemination areas, and Create an ETA Vector;
    Disseminate the ETA Vector in each sector towards dissemination areas;
    if *(EmV arrived)* **then**
      Clear/Delete the previous dissemination area; Stop;
    end
  end
end

The reference scenario shown in Fig. 1 and Fig. 3 is modeled as a graph that consists of route nodes and WPs. The sequence of the WPs (i.e., WP_1, WP_2,...WP_i) defines the size, and the edges of the dissemination areas, and it represents the route-path that the EmV should follow.

Estimating the time of arrival for different dissemination areas is based on the EmV's current location with reference to each WP (i.e., WP_i), and it is denoted as ETA_i. The sum of all travel times of consecutive WPs is considered to be the total time of travel.

According to Min et al. [18], the time of arrival (i.e., ETA_i) for each dissemination area follows a probability density function $F_i(t)$ with a mean value $\mu(t_i)$ and a variance $\sigma(t_i)^2$, and depicted in equations (1) and (2) respectively.

$$\mu(t_i) = \int_{t_1}^{t_N} tF_i(t)dt \tag{1}$$

$$\Big(\sigma(t_i)\Big)^2 = \int_{t_1}^{t_N} t^2F_i(t)dt - \left(\int_{t_1}^{t_N} t^2F_i(t)dt\right)^2 \tag{2}$$

The time t_1 in equation (2) represents the starting time of the trip, while t_N denotes the time of reaching the destination. As expressed in equation (2), the variance of the time of arrival for a specific segment of the dissemination area is not constant. In fact, it is dependent on various factors, such as delay, changes of the speed, stops, weather, and any prevalent traffic

conditions. The information about the variance calculated in equation (2) is used by the present systems to select the shortest path to the destination by minimizing the mean and the variance of ETA_i [18], but our proposed system overcome this. As indicated above, our proposed BSA service ensures in-advance notification of the EmV arrival time, therefore it is expected from the vehicles in front to free the requited lane for the EmV. In this new situation, the proposed system can always select the shortest path excluding traffic conditions, time of day/year, or other impact factors.

As denoted in equation (3) (see [18]), the ETA (t_{i+1}) is calculated with reference from EmV's current position to a specific WP (WP_{i+1}), and thus depends on the ETA (t_i) for the previous WP, (WP_i), the average speed of the EmV ($s_{v_i,v_{i+1}}(t_i)$), as well as the distance between two successive WPs ($L_{i,i+1}$).

$$t_{i+1} = t_i + \frac{L_{i,i+1}}{s_{v_i,v_{i+1}}(t_i)}. \tag{3}$$

The distance is a constant parameter and depends on the route-path that the EmV selects to reach the destination. It is calculated using the WPs obtained from the MEC Map service (see Fig. 3) along the selected route-path. Following this fact, we assume that the variance of the ETA depends only on the average speed of the EmV.

The average speed of the EmV, i.e., $s_{v_i,v_{i+1}}(t_i)$, refers to the value of speed maintained between two successive WPs, i.e., WP_{i+1} and WP_i, and it is obtained considering the historical data of previous traveling experiences on the same route-path. For obtaining the historical data on speed, we relied on a dataset collected from field measurements as explained in the next section. In our previous work [9] we used historical data to have the actual speed of the EmV derived from the periodically received CAMs for ETA estimation using the Kalman filter. In this work, we added more experimental measurements and analysed three additional approaches namely i) Filter-less method, ii) Simple Moving Average Filter, and iii) Exponential Moving Average Filter. The key objective of assessing the different filtering methods is to analyze them for accuracy and their feasibility in terms of the algorithm complexity. For realistic assessment of the reference algorithms, we utilize the dataset that is collected from the field measurements of the vehicle driving on the Smart Highway testbed that is installed on the E313 highway in Antwerp, Belgium [39]. More details on the testbed is provided in Section V.

In this work, we assume that changes in speed that are reflected in the datasets are caused by weather conditions, traffic congestion, and ridership. Hence, all of these impact factors are used. The speed parameter is obtained by the GNSS device that reports position, speed, and time when this sample data is recorded. The speed parameter values are updated while the vehicle is driving on the study path with the transmission frequency of 1 Hz. According to our analyses we consider this value as high enough to enable our methods to derive outputs within acceptable bounds of ETA estimation error. Further details on error bounds are provided in Section V-B

B. Overview of the reference methods

To compare and assess the resulting ETA accuracy, four different forecasting methods are used.

1) Filter-less method: When using filter-less method, a single EmV speed value (v[n]) obtained from a single CAM notification received (without taking into consideration the previous speed data), is considered to have the ETA.

In such case the ETA in the equation 3, respectively the average speed $s_{v_i,v_{i+1}}(t_i)$, via a discretized method will be

$$s[n] = v[n]. \tag{4}$$

In such instances, anytime the BSA application receives a CAM notification, it will consider the EmV reported speed $v_i(t_i)$ (or v[n]) and will calculate the ETA value for the upcoming way-points on the highway while the EmV is reaching the emergency case.

2) Simple Moving Average Filter: Simple Moving Average, as the name indicates is an average that moves. The average is created using older data in combination with the new available data, causing this parameter to move along the time scale.

When using this method, the speed parameter s[n] is formed by computing the average speed of the EmV over a specific period, which we define as windows size. In our case we have considered a window size (N) equal to 5, which means that the average speed $s_{v_i,v_{i+1}}(t_i)$ in equation 3 is based on the last five speed values reported by the EmV.

$$s[n] = \frac{1}{N} \sum_{i=0}^{N-1} v[n-i]. \tag{5}$$

As shown on the equation 5 the average speed using the Simple Moving Average filter is derived from the sum of the values divided by the number of values.

3) Exponential Moving Average Filter: Exponential Moving Average Filter, same as the Simple Moving Average follows the moving average logic too. However, in this case the resulted average speed depends on the previous average and the current speed value. The filter is called 'exponential', because it uses an exponentially smoothing factor α to include the weight of previous inputs speed values, equation 6.

$$s[n] = \alpha \sum_{i=0}^{N} (1-\alpha)^i v[n-i]. \tag{6}$$

4) Kalman filter: As reflected in the literature [10,16,40,41], the Kalman filter has been used extensively in numerous areas with practical applications. In particular, it is usually applied to model the systems that are characteristic for multiple inputs and output parameters, considering both stationary and non-stationary situations [16]. This filter consists of the initialization, prediction, and correction steps, for every input value, and it uses linear stochastic difference equations to estimate values of interest [42]. As shown in the equation (7), $\underline{x}_k$ is the state variable, which is in our simulation case the ETA. Then, A is the state transition constant, which relates the present state $\underline{x}_k$ of the ETA to its previous state $\overline{x}_{k-1}$. Since ETA is a one-dimensional value, A is equal to 1.

$$\underline{x}_k = A\overline{x}_{k-1} + Bu_{k-1}. \tag{7}$$

Furthermore, the parameter B associates the control input u parameter to the ETA value. Since the ETA value is one-dimensional, the same rule applies to B, and it is equal

to 1. The control input u is a vector and it is modeled using the aforementioned real data measurements. Thus, it is included in the recorded average speed for the considered dissemination areas. In order to include the impact of different traffic changes, we consider the process noise covariance Q, thereby obtaining the covariance matrix P_k.

$$\underline{P}_k = A\overline{P}_{k-1}A^T + Q. \tag{8}$$

For the correction step, we consider the real data measurements and follow the equations (9)-(11). In our case study, the measured historical average speed values are used to have the vector of the ETA measurement values expressed as z_k. H is the transformation matrix, in our case is 1, and $\underline{x}_k$ is obtained using the above mentioned mapping system. Obtained measurements include noise or uncertainty, whose variance is R. The Kalman gain K, expressed in equation (9), determines to what extent the predictions should be corrected in time step k. This estimation/prediction error is the difference between the predicted value and the actual measurement. Depending on the value of variance measurement noise R, this gain gives weight to the predicted or the measured value. A large value of R results in the small K, which means that the predicted value does not reflect the measured one. On the contrary, if R is small, it means that the measurements for the specific area are approximated with an insignificant error value.

$$K_k = P_k H^T (H\underline{P}_k H^T + R)^{-1}. \tag{9}$$

$$\overline{x}_k = \underline{x}_k + K(z_k - H\underline{x}_k). \tag{10}$$

$$P_k = (I - K_k H)\underline{P}_k. \tag{11}$$

To get the input value of R, we have obtained the difference between time intervals or time of arrival recorded by the Global Navigation Satellite System (GNSS) receiver while driving in the highway, and the time of arrival calculated using the mapping system and recorded speed by the device. The error values vary between minimum 0.00 s to 0.46 s as maximum, with the mean value of 0.00 s, a standard deviation of 0.20 s, and a variance 0.041 s. This result is used on the simulation of the ETA calculation.

C. Dissemination area size determination

As described above, the BSA service determines the EmV's ETAs with reference to different WPs along the route-path, and then disseminates the calculated ETA values in respective dissemination-areas. A dissemination-area is defined as a region between two successive WPs, and the ETA is derived with reference to the WP marking the beginning of each dissemination area. Thus, all vehicles within the respective dissemination area will receive the same ETA value. As a results, despite the prediction error which is an outcome of the above mentioned forecasting techniques, the ETA value within a dissemination area (i) will have another estimation error ($e(t_i)$) which will depend on the size (i.e., road-length) of the dissemination area (L_i).

In our previous work [9] we gave an empirical evidence of the effect of dissemination area size expressed by L on the estimation error (e_i), which is shown in Fig. 5 using reference dissemination area size of 250m, 500m and 1000m. From this figure [9], it is observed that the lowest of the maximum estimation error of 62.22s is for L=250m as compared to 92.10s observed for L=500m, with the highest maximum estimation error of 118.08s observed for L=1000m. Comparing the average values, we have 25s for L=250m, 23.32s for L=500m, and 31.42s for L=1000m being the largest average estimation error [9].

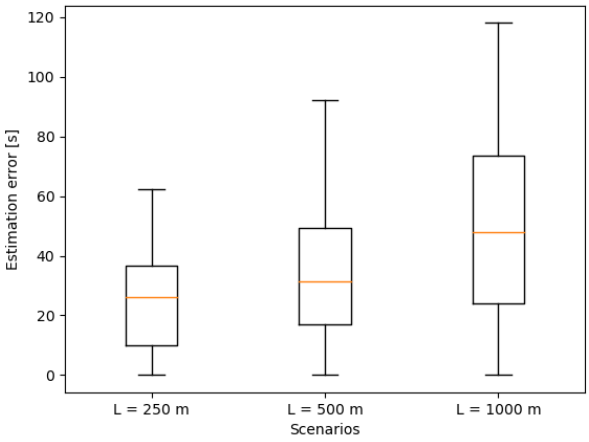

Fig. 5: Variation of the estimation error for Scenario 1 (L=250 m), Scenario 2 (L=500 m) and Scenario 3 (L=1000 m) [9].

As we can see the higher dissemination area size produces larger error. The error behaviour and its dependency on the dissemination area size is used to model, predict, and to limit it under a defined threshold suitable for an emergency situation. In this regard, our analysis and observations of the data acquired from the real experimental drives performed on the E313 highway in Belgium presented in next section, show a relation between estimation error ($e(t_i)$) of the ETA value, dissemination area size (i.e., road-length) ($L_(t_i)$), the speed of the EmV ($v(t_i)$) and an index ($n(t_i)$), and this is expressed in equation 12. The index n reflects the traffic conditions, weather conditions, time of the day/year, and other parameters that may impact the speed of the EmV.

$$e(t_i) = f(L(t_i), n(t_i), v(t_i)). \tag{12}$$

Fig. 6 illustrates the impact of the size of the dissemination area (L_i) on the estimation error, where the dissemination area is defined between WP-1 and WP-2. The figure shows that the magnitude of error value is proportional to the size of the dissemination-area $DA-1$, $DA-2$, $DA-3$, characterized by a linear increase in the estimation error as the size of the dissemination area increases from L_1 to L_2 to L_3 respectively. The slope of the estimation error is a positive and is defined by the change in the actual time of arrival (ATA) parameter divided by the corresponding change in the distance parameter, between two distinct points on the highway segment. Intuitively speaking, within a dissemination area, the ETA error will be pronounced for vehicles that are farther away from the reference WP (i.e., WP_1 in Fig. 6).

According to our analysis and observations of the data acquired from the real experimental drives performed on the

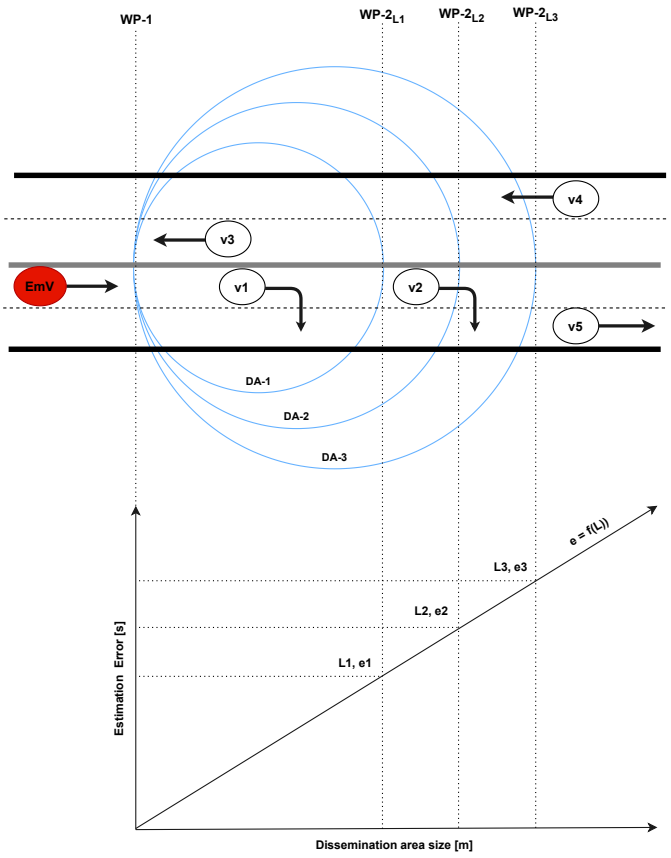

Fig. 6: Estimation error e dependency on the dissemination area sizes L.

E313 highway in Belgium, the index n has a mean value of 1.06, minimum 0.83, maximum 1.41, and a standard deviation of 0.16. Furthermore, this index has a tendency to exhibit very small changes between two successive ETAs calculation, thus has negligible effect on two successive errors estimations. This makes it possible to use the previous value of the estimation error index $n(t_i)$ for the proceeding estimation error index $n(t_{i+1})$.

Therefore, for every periodically CAM received, we use the relation between actual time of arrival ATA_i, speed of the vehicle $v(t_i)$, and the traveled distance d_i, obtained at the time t_i as represented in equation 13, to forecast the index n for the upcoming time t_{i+1}.

$$n(t_{i+1}) = ATA_i \frac{v(t_i)}{d_i}. \tag{13}$$

The dynamically changing index n from every periodically CAM received is dynamically mirrored on the dissemination areas sizes $L(t_{i+1})$ determination (see equation 14), so the estimation error caused by this size stays under a defined threshold (e_{i+1}^{max})

$$L_{i+1}^{max} <= e^{max}(t_{i+1}) \frac{v(t_i)}{n(t_{i+1})}. \tag{14}$$

The numerical value of the threshold $e^{max}(t_{i+1})$ is the maximum estimation error allowed at the end of the generated dissemination areas (i.e., numerical value of e_1 if L_1 is selected, or e_2 for L_2, or e_3 for L_3, in Fig. 6). As shown

Fig. 7: The segment of the two way E313 highway in Antwerp, Belgium. © 2020 Google.

on the Section V-B, since the EmV will constantly move and update the system with CAM notifications, vehicles will receive updated values of the ETA, so this will not cause traffic problems.

V. Performance Evaluation

We evaluated the performance of the BSA application using a simulation of the case study presented in Section III by including 4 reference methods in terms of accurate estimation of ETA, analysing the parameters that impact this ETA accuracy, and by using real data measurements presented below in this section.

A. Experimental testbed for reference data collection

In order to analyse the performance of the 4 reference methods in terms of accurate calculation of ETA, a real dataset was used as reference. As shown above this dataset consists of test data that has been acquired by a test vehicle driving on the selected segment of the E313 highway in Antwerp, Belgium (see Fig. 7) where the Smart Highway Testbed is installed. Besides other parameters, the test data captures the ATA of the test vehicle.

The testbed infrastructure considered consists of the interconnected hardware entities, including: a vehicle equipped with an Onboard Unit (OBU), the backbone, the testbed management software platform, and the optical fibre ring along the E313 highway.

As shown in Fig. 8a, one part of the OBU is placed 1.8 m high on the vehicle roof and contains an accurate GNSS module AsteRx-m2a with RTK correction, and two GNSS PolaNt-x MF antennas. The second part of the OBU, shown in Fig. 8b is placed inside of the vehicle and contains a processing unit with an independent power system, which can power the OBU for several hours.

This device records the position of the vehicle expressed by its latitude and longitude with a predetermined frequency, the time-stamp when this position is obtained, precise and reliable heading information, and the vehicle's speed. These parameters are identified using an ID and are stored for post-processing.

Data measurements are obtained at different hours of the day, months, and years, so we can evaluate the ETA performance under diverse traffic conditions. The travel-time data are collected in November 2020, (2020-11-19, 14:00 to 17:00 CET), June 2019 (2019-06-18, 14:00 - 15:00 CET), and July 2019, (2019-07-17, 12:00 to 14:00 CET).

Figure 9 shows the sample of 10 test drives in terms of the vehicle's positions (Fig. 9a) and the time-stamps at the respective positions (Fig. 9b). The vehicle's position corresponds to the position of the OBU recorded by the GNSS device, and

(a) The OBU Roof Unit mounted on the roof together with the GNSS antennas.

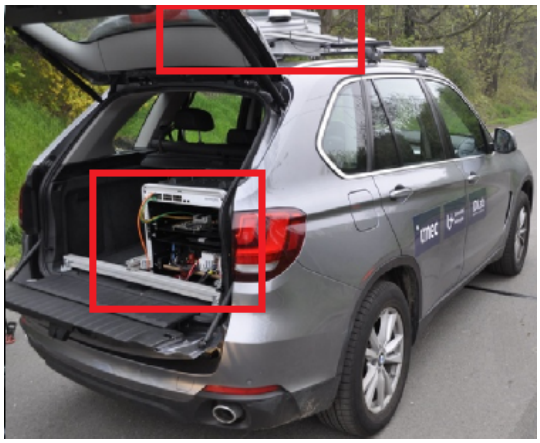

(b) The OBU Roof Unit placed on the vehicle roof and the OBU Car Unit placed inside of vehicle.

Fig. 8: The OBU placed on the vehicle.

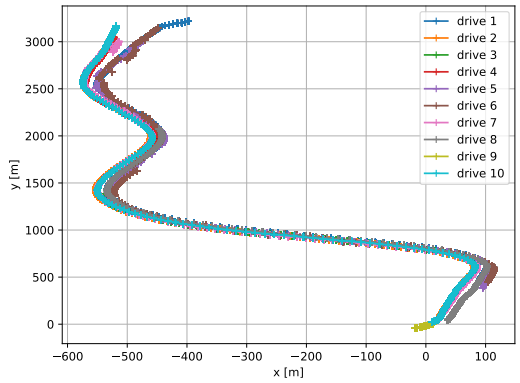

(a) Positions of the OBU while driving on the E313 Highway

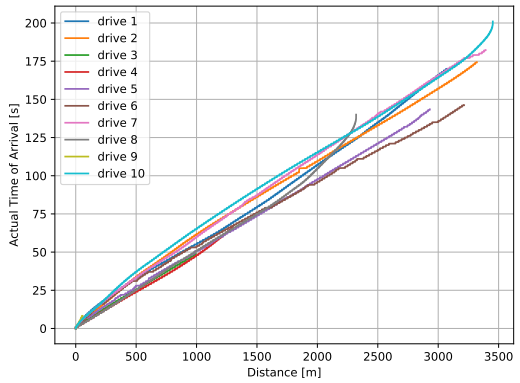

(b) Real measured travel time, referred as Actual Time of Arrival of the OBU while driving on the E313 Highway

Fig. 9: Map of the OBU drives on the E313 Highway and their real time of arrival depending on the distances from the start to the destination.

is shown in Fig. 9a as x and y coordinates as a transform of the geodetic coordinates specified by latitudes, longitudes, and height to the local north-east-down Cartesian coordinates specified by xNorth, yEast, and zDown.

Fig. 9b reflects the time-stamp for each recorded position, which will be used as the Actual Time of Arrival (ATA) of the vehicle in our algorithms and analysis. As can be seen, the speed of the OBU changes resulting in different arrival times in different sections or distances from the starting point.

B. Results and Analysis

The main purpose of this work was to evaluate the performance of the BSA algorithm in terms of the following key objectives:

1) Comparing the performance of the four reference methods in terms of accurate ETA calculation.
2) Determining the dissemination area size in order to obtain ETA estimation errors under an acceptable limit.
3) Analysing the impact of the CAM input frequency on the ETA estimation error.

For the performance analysis, we use KPIs such as minimum/maximum/average/standard deviation of the estimation error. In addition to this, we use three KPIs to measure the prediction accuracy of the forecasting methods or estimators when compared to the values observed (ATAs).

Mean Absolute Error (MAE) is used to obtain the natural average magnitude of the absolute estimation errors by giving the same importance to each error. Mean Absolute Percentage Error (MAPE) is used to express accuracy as a percentage of the error. It is the sum of the individual absolute estimation errors compared or divided with the respective ATAs. Root Mean Square Error (RMSE) is used to include and give importance to the most significant estimation errors or higher deviations from the observed values. Thus, by considering these three KPIs we have a complete picture of the estimation error distribution.

The data sets obtained from the field tests described in the subsection V-A are used to analyze the difference between the ATAs and the ETAs as computed by the four reference methods and thus compared as to which method provides a more accurate ETA estimation.

As indicated above, for every received CAM notifying the current location and speed of the EmV, the algorithm generates ETA values for the whole EmV expected journey. Figure 10 presents the generated ETA values for all points till the destination based on the information received from the first CAM notification only. In this figure we compare the predicted values (ETAs) derived using four reference methods with the real-time of arrivals (ATAs) recorded by the GNSS receiver, when the EmV is located at the starting point of the journey and has a long distance in-front toward the destination. For the ATAs we have used one of the OBU drives shown in the Fig.9b.

As expected, the quality of prediction degrades over distance

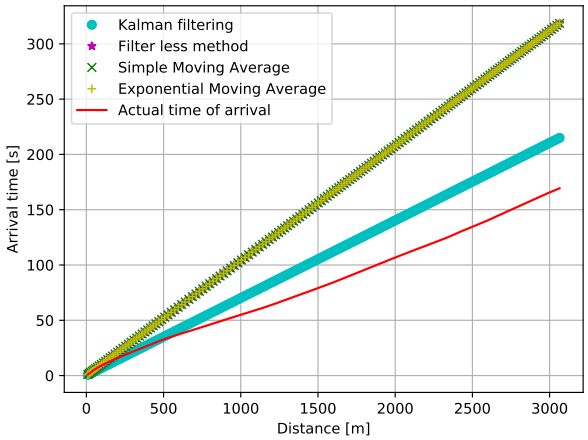

Fig. 10: Comparison of the real measured travel time ATA and the ETA values derived using four reference methods and information received from the first CAM notification only.

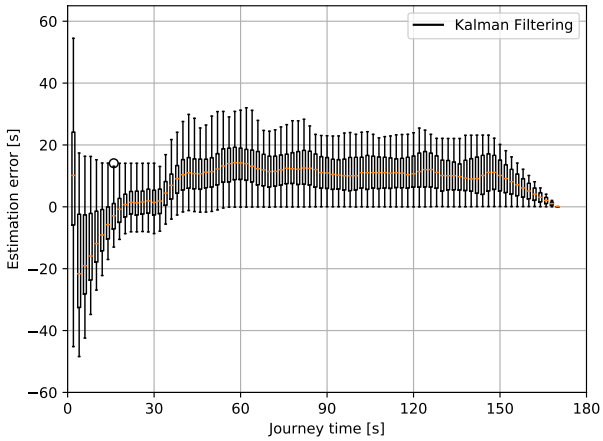

Fig. 11: Estimation errors obtained on different locations/distances toward the emergency case when using Kalman filtering.

and it diverges more and more away from the ATAs. We can see that all methods overestimate the arrival time of the EmV for the area above 600m away from the EmV current location. In this situation the vehicles at the front will experience the presence of the EmV much earlier than the notified ETA time, thus giving drivers limited opportunity to safely manouver away from the EmV's path. Our solution avoids this scenario, since our algorithm is constantly updated with the CAM notifications, which ensures the update of ETA values too. This process increase the ETA accuracy by specifying several WPs along the route path and the distance between successive WPs (i.e., dissemination area), which is also dynamically adjusted in order to keep the ETA estimation error below a specified threshold.

From the Fig. 10, it is observed that the predicted values of the ETA derived when using the Kalman filter follows more closely the ATA values obtained on the highway compared with other three reference methods, which have very similar outputs. Here we can clearly see the importance of the adaptive and self-correcting feature of the Kalman filtering that adjusts itself during the drive, a feature that is not present in the other 3 reference methods.

The difference between the recorded ATAs and the respective generated ETAs results in a vector containing estimation error values. This vector contains a maximum, minimum, average, and standard deviation values that characterises error values. How the maximum, minimum, average, and standard deviation for all estimation error vectors change during the entire journey time of the EmV, until it reaches the target destination is shown in Fig.11 (for better visibility results are plotted every 2 seconds). In this case the algorithm is updated with 1Hz frequency of input data and uses Kalman Filter for prediction.

For every box plot representing the resulted vector in Fig.11 we see the peaks of estimation errors (positive and negative). As observed these predictions errors peaks are obtained for locations/distances far in-front from the EmV's current locations. This can be seen and is described in Fig. 10. The algorithm is very accurate for short distance predictions (area under 1km distance from the starting point in Fig. 10), thus the estimation error values are very low, however, when the prediction distance increases the estimation error values increase too (area above 1km distance from the starting point in Fig. 10). Since the algorithm is constantly updated with new CAM notification, the ETA accuracy is constantly updated and improved as well. This is the first advantage of our solution compared to existing systems. Also, while the EmV moves forward toward the target destination, the prediction distance decreases, therefore the estimation errors decreases too. This is reflected in Fig.11. While reaching the end of the journey the range of the estimation errors gets smaller (especially on the last area, journey time between 150s and 180s).

A comparison of the estimation errors' peaks obtained using Kalman filtering, Filter-less method, Simple Moving Average Filter, and Exponential Moving Average Filter is presented in Fig. 12a. Additionally, a comparison between the 4 approaches is presented using Mean Absolute Error (see Fig. 12b) and Root Mean Square Error (see Fig. 12c). All these KPIs are shown for the whole distance or for the whole journey time that the EmV travels toward the intended destination. The results show that the Kalman Filter exhibits a much lower estimation errors as compared to the other three reference techniques. Also, all methods increase the prediction accuracy while the distance toward the target destination decreases.

More details about numerical results for four differed considered techniques using four different reference scenarios with reference to the EmV location or distance from the staring point are found in Table II.

When the EmV sends the first CAM notification at the start of journey at position d_0, the maximum estimation error which we obtain is 54.46s for Kalman filtering and 147.57s for other methods. At this time the MAPE is 41%, if the Kalman filter is chosen, and 62% for other techniques (see Table II). Apparently, the estimation using a Kalman filter performs better with the percentage error reduced by 21%, from 62% to 41%. The estimation error comparison for all reference points shows that there is a 21% error reduction when the EmV is found at d_0, (11-13)% at d_1, (8-10)% at d_2, and (6-8)% at d_3, when using Kalman in comparison with

TABLE II: Comparison of the estimation error obtained at d_0, d_1, d_2, d_3 using different techniques and different performance criterion.

Distance traveled d_i, Dissemination area size L	Prediction Technique	Min	STD	Max	Average	RMSE	MAE	MAPE (%)
d_0=9.5m, L=1000m	Kalman Filtering	0.072	21.94	54.46	9.38	23.86	19.55	41
	Filter less method	0.009	47.02	147.57	-27.15	54.30	44.77	62
	Simple Moving Average	0.009	47.02	147.57	-27.15	54.30	44.77	62
	Exponential Moving Average	0.009	47.02	147.57	-27.18	54.30	44.77	62
d_1=710m, L=335m	Kalman Filtering	0.086	7.00	28.90	11.33	13.32	11.38	20
	Filter less method	0.009	9.50	37.48	16.98	18.42	16.04	31
	Simple Moving Average	0.015	9.16	37.92	-27.15	18.68	16.28	33
	Exponential Moving Average	0.004	8.91	36.99	15.77	18.12	15.77	33
d_2=1598m, L=380m	Kalman Filtering	0.012	6.44	24.64	12.15	13.75	12.36	25
	Filter less method	0.010	6.44	24.55	12.10	13.71	12.10	33
	Simple Moving Average	0.040	6.64	26.43	-27.15	14.66	13.07	35
	Exponential Moving Average	0.035	6.60	26.11	12.90	14.49	12.90	34
d_3=2361m, L=375m	Kalman Filtering	0.061	6.40	22.15	11.57	13.22	11.57	29
	Filter less method	0.014	6.38	22.05	11.03	12.74	11.03	35
	Simple Moving Average	0.071	6.41	22.39	-27.15	13.34	11.70	37
	Exponential Moving Average	0.06	6.40	22.13	11.65	13.22	11.66	36

other methods.

Maximum values, MAE, and RMSE shown in Fig. 12 show that the Kalman filter performs better, considering the entire travel time, while we notice a relatively small difference on estimation error values between the other three methods. Same observation is shown in Table II using standard deviation, mean value, minumum and maximum values, MAE, MAPE, and RMSE for 4 reference positions considered.

Moving to the second objective of this work, it is important to stress that, in addition to estimation errors inherently caused by the considered filtering methods, the dissemination area size also has an impact on the magnitude of the estimation error.

The fact that we share one ETA value for all cars which are found within a dissemination area, estimation error has the lowest value at the start of the dissemination area (i.e., between two successive WPs) and it increases successively as it reaches the end of the respective dissemination area (i.e., until it reaches the starting point of the next dissemination area).

In our case, at the first step the dissemination area size is a default value, equal to 1000m, and then its size changes according to the speed value extracted from a periodic CAM notification and the upper error limit or threshold (see eq. 14). As a result, on the second, third, and upcoming CAM notifications and derivation of the ETA values increases accuracy. Referring to Kalman filtering results, on the second CAM notification the minimum estimation error tends to be zero and the maximum error is around 18s at the end of the first dissemination area (determined or limited by the threshold value), and 47s at the end of the journey (in our case more than 3km far form the current EmV location). Although the error is 47s for the end point of the journey, each new derivation of ETA will improve accuracy, and civilian cars will receive updated messages with updated values of ETA for their respective dissemination areas.

Therefore, as concluded in Section IV-C, the estimation error is a function of dissemination area size L, speed v, and the n index, thus we can predict, control, and bound this error by operating with the aforementioned parameters (eq. 12). To better showcase this we present the behavior of the estimation error at four considered reference EmV locations (see Figure 13). For all cases considered, including here four reference scenarios with reference to the distances form the starting point selected as d_0, d_1, d_2, and d_3, and four techniques used, are provided and compared numerical results of the estimation errors (Fig. 13 and Table II) and their Cumulative Distribution Function (CDF) (Fig. 14)

When the EmV was at d_0, Fig 13a, the dissemination area sizes were 1000m (used as a starting default value), and in this case the RMSE for Kalman filtering is 23.86s, while it is 54.30s for other three techniques. Then, when the EmV moved and reached d_1 or traveled 710m from the starting point, Fig. 13b, our algorithm adjusts the dissemination area size in order to decrease the estimation error, thus the new size becomes 335m, while the RMSE of the estimation errors are found to be 18.42s for Filter-less method, and 18.68s for Simple Moving Average Filter, and 18.12s for Exponential Moving Average Filter, compared to Kalman filtering 13.32s. This clearly shows that the adjustments in the self-correcting algorithm decrease continuously the estimation error. Fig. 13c and Fig. 13d are cases when the EmV moved further to d_2 equal to 1598m distance, respectively d_3 equal to 2361m distance from the starting point, and the dissemination area sizes were rounded as 380m, respectively 375m, while the obtained results support the previous conclusions. Again, Table II can be used for other KPIs comparison, respectively minimum, maximum, mean, standard deviation, MAE, MAPE of estimation errors. The respective CDF results in Fig. 14a, 14b, 14c, 14d, echo the above conclusions.

With the dynamic adjustments of dissemination area sizes, applied by extracting the EmV's speed from the received CAM, as well as the maximum allowed error (threshold), our algorithm is capable of providing more accurate ETA estimations. This is the second advantage of our solution compared to the existing systems.

Analyzing all four sample cases with reference to the distances passed by the EmV from the starting point (d_0, d_1, d_2, and d_3), for all considered techniques in this study, it is evident that the rise in estimation error is smaller for Kalman filtering compared with Filter-less method, Simple Moving Average Filter method, and Exponential Moving Average Filter method. Also we see that the estimation error is decreasing as the EmV approaches the target destination. As we discussed earlier in this section, this decrease in estimation

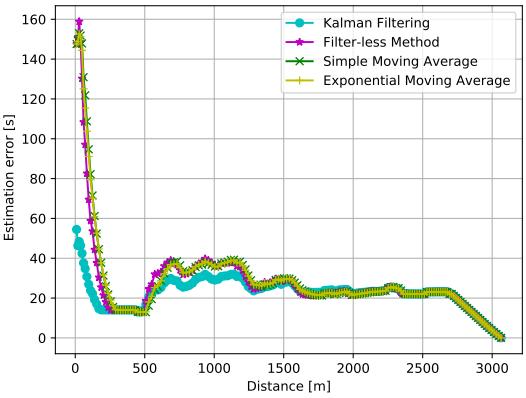

(a) Maximum estimation error values.

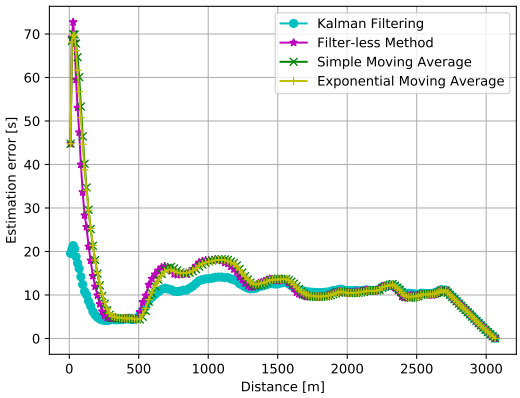

(b) Mean Absolute Error values.

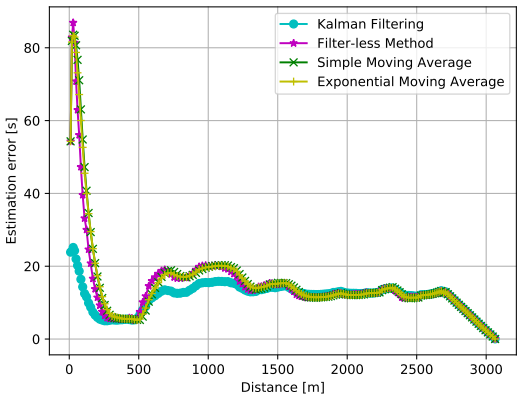

(c) Root Mean Square Error values.

Fig. 12: Comparison of the estimation errors obtained on different locations/distances toward the emergency case for the considered techniques and for the entire journey.

error occurs due to self-correcting nature of our algorithm that constantly considers the updated CAM data and dynamically adjusts dissemination area size, but also due to the prediction distance from the destination, which is getting shorter as the vehicle moves forward.

In addition to this, we explored the variations we received when we changed the window sizes of the average speed as input data for Moving Average filter (eq. 5) and Exponential Moving Average filter (eq. 6), from 5s to 10s, and 50s. The results obtained when changing the windows size does not show an improvement compared to Kalman filtering. On the contrary, for some locations on the case study, averaging speed values for longer intervals produced an underestimation of the EmV arrival time.

It is important to recall that in this new proposed solution, vehicles will receive early notification of an approaching EmV, thus they will clear the required lane. In this new situation the EmV can always select the shortest path or/and the path where it can drive at the maximum allowed speed for emergency systems, thus there is no need for long time speed data history to provide an accurate ETA calculation. This is the third advantage of our solution compared to existing systems.

As presented on the third objective of this work, we included results we obtained when changing the input CAM frequency. Here it is evident that the CAM frequency affects the estimation error due to the more granular input data. Fig 15 shows the results obtained when changing the CAM period from 0.1s, to 1s, 2s and 3s. It is observed that increasing the period of CAM generation or decreasing the CAM frequency results with higher estimation errors. However, the difference in maximum MAE values, when different CAM frequencies are considered is less than 2 seconds. Such small value does not affect the performance of BSA, because the MEC service sends periodic updates to the vehicles in a timely manner, i.e., early enough to clear the lane. For example, if notification for a civilian vehicle indicates that an EmV is approaching in 2 minutes (which is an ETA value), and EmV arrives in 2 minutes and 2 seconds or 1 minute and 58 seconds, it would not affect the driver's decision to clear the lane. According to study provided in [43], the average duration of lane change on the highways is 5.8s, which means that driver will need to make a plan on the lane change upfront, and 2 seconds will clearly not play a significant role in this decision.

Finally, we observed the computational time complexity of the Kalman Filter compared to other methods. The Kalman Filter, as explained above, it has initialization, prediction, and correction steps, for every input value. It has a recursive nature, which means it uses the output as an input to the next calculation. This increases computational time compared to the other three methods considered in this study. However, as seen in the Fig 15, Kalman filter sustains better stability on the accuracy compared to other methods when the CAM period increases from 1s to 2s, and 3s. So, choosing between longer computational time vs better prediction results, we consider it is better to have better prediction results since the changes in the computational time are not relevant for an emergency situation.

VI. Conclusion

In this paper we introduced the BSA application for providing an early notification of the ETA of an approaching EmV. The ETA is calculated by the BSA service placed within the MEC system. As the ETA algorithm provides the main logic to the BSA application, the performance of this self-correcting algorithm has been analyzed and evaluated in terms of achievable accuracy of ETA, by incorporating dynamic dissemination area size and use of different forecasting techniques. The real

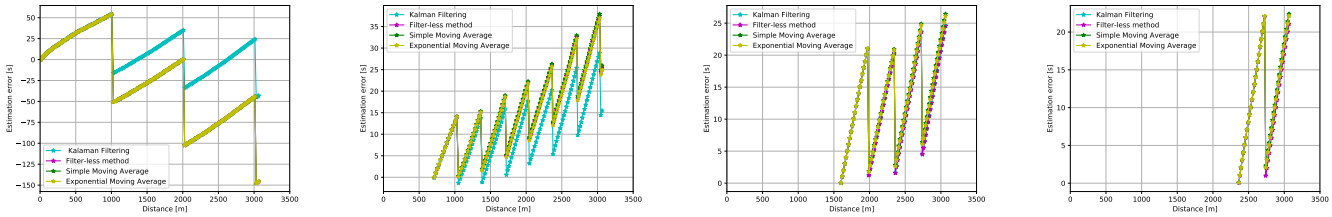

(a) e, $\mathrm{d}_0 = 9.5m, L = 1000m$. (b) e, $\mathrm{d}_1 = 710m, L = 335m$. (c) e, $\mathrm{d}_2 = 1598m, L = 380m$. (d) e, $\mathrm{d}_3 = 2361m, L = 375m$.

Fig. 13: Comparison of the estimation errors for different dissemination areas size.

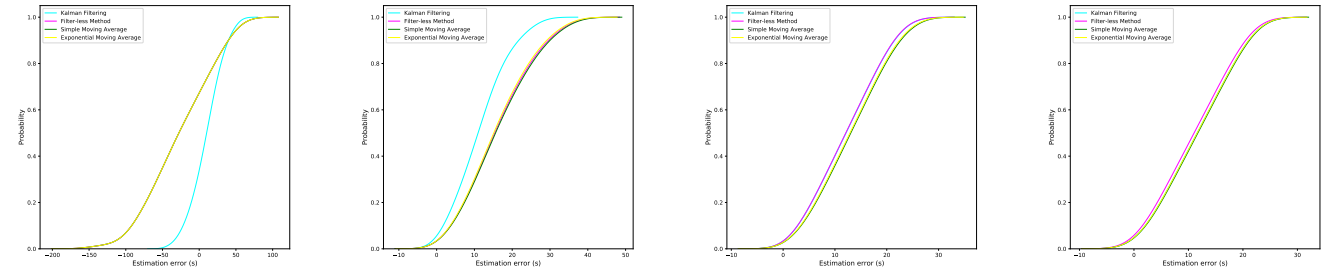

(a) CDF at d_0. (b) CDF at d_1. (c) CDF at d_2. (d) CDF at d_3.

Fig. 14: CDF for estimation errors in case of different dissemination areas size.

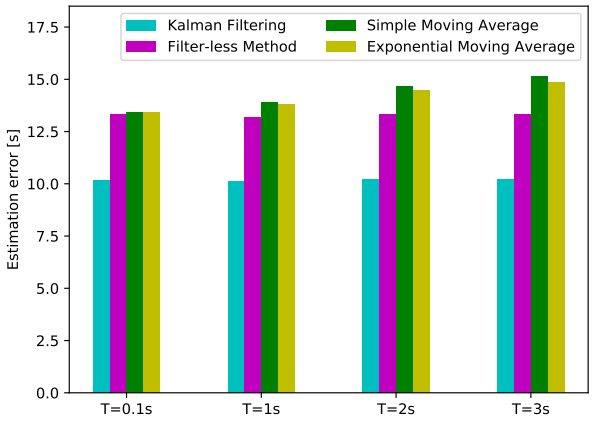

Fig. 15: Comparison of the MAE maximum values obtained for the whole journey of the EmV using different period T for CAM notifications.

field data measurements obtained in a realistic environment, in Smart Highway testbed in Antwerp, Belgium, are used for evaluation and comparison.

First, the developed algorithm is periodically updated with the EmV speed and location information, to follow the flow and fast changes in the traffic, and it uses these inputs for its self-correcting behavior to improve the ETA accuracy.

Second, the developed algorithm analyses the dependency between estimation error, dissemination area size, and the EmV speed while heading to the emergency case. As a result, it provides the concept of dynamic dissemination area size allocation. This newly added feature to our proposed BSA algorithm maintains the estimation error under a defined threshold, required for an emergency situation.

Using two above innovative application features, a comparison between Kalman filter, one step speed values from CAM referred as Filter-less method, average speed values using Moving Average filter, and Exponential Moving Average filter, is performed to derive conclusions regarding the methods capability to provide more accurate ETA estimation and lower estimation error. According to our results, the Kalman filter proved to produce the best result by providing the highest estimation accuracy, comparing to the other prediction methods. This Kalman accuracy gain becomes even more relevant when the algorithm needs to predict for long distances in-front.

The computational time complexity of the Kalman Filter is higher compared to other methods because of its recursive nature, however, it has the same order of magnitude hence the increase in time is not significant.

In this new situation when the ETA notification is beyond the audio and visual range of the EmV, drivers have enough time to take the required actions and clear the lane, the EmV can always select the shortest path toward the destination and drive at the maximum allowed speed for emergency systems, by constantly being updated with traffic changes. As a result, the proposed solution is expected to not only improve the road safety standards, but also enhance the mission success and response time of emergency responders.

ACKNOWLEDGMENT

This work has been funded by the European Union Horizon-2020 Project 5G-CARMEN under Grant Agreement 825012. The views expressed are those of the authors and do not necessarily represent the project.

REFERENCES

[1] R. Aringhieri, G. Carello, and D. Morale, "Ambulance location through optimization and simulation : the case of milano urban area," 2007, doi: http://dx.doi.org/.

[2] R. Sánchez-Mangas, A. García-Ferrrer, A. de Juan, and A. M. Arroyo, "The probability of death in road traffic accidents. how important is a quick medical response?" *Accident Analysis & Prevention*, vol. 42, no. 4, pp. 1048–1056, 2010, doi: http://dx.doi.org/10.1016/j.aap.2009.12.012.

[3] R. B. Vukmir, "Survival from prehospital cardiac arrest is critically dependent upon response time," *Resuscitation*, vol. 69, no. 2, pp. 229–234, 2006, doi: http://dx.doi.org/10.1016/j.resuscitation.2005.08.014.

[4] M. Poulton, A. Noulas, D. Weston, and G. Roussos, "Modeling metropolitan-area ambulance mobility under blue light conditions," *IEEE Access*, vol. 7, pp. 1390–1403, 2019, doi: http://dx.doi.org/10.1109/ACCESS.2018.2886852.

[5] N. Smith, "A National Perspective on Ambulance Crashes and Safety - Guidance from the National Highway Traffic Safety Administration on Ambulance Safety for Patients and Providers," *EMS Report*, 2015, online [Available]:https://pubmed.ncbi.nlm.nih.gov/26521402/.

[6] K. Donoughe, J. Whitestone, and H. Gabler, "Analysis of Firetruck Crashes and Associated Firefighter Injuries in the United States," *Annals of advances in automotive medicine / Annual Scientific Conference. Association for the Advancement of Automotive Medicine. Association for the Advancement of Automotive Medicine. Scientific Conference*, vol. 56, pp. 69–76, 10 2012, online [Available]:https://www.ncbi.nlm.nih.gov/pmc/articles/PMC3503424/.

[7] ETSI, "Mobile Edge Computing - A Key Technology Towards 5G," *ETSI White Paper No. 11*, no. 11, 2015, online [Available]: https://www.etsi.org/images/files/ETSIWhitePapers/etsi_wp11_mec_a_key_technology_towards_5g.pdf.

[8] F. Z. Yousaf, M. Bredel, S. Schaller, and F. Schneider, "NFV and SDN—Key Technology Enablers for 5G Networks," *IEEE Journal on Selected Areas in Communications*, vol. 35, no. 11, pp. 2468–2478, 2017, doi: http://dx.doi.org/10.1109/JSAC.2017.2760418.

[9] R. Halili, F. Z. Yousaf, N. Slamnik-Kriještorac, G. M. Yilma, M. Liebsch, E. de Britto e Silva, S. A. Hadiwardoyo, R. Berkvens, and M. Weyn, "Leveraging mec in a 5g system for enhanced back situation awareness," in *2020 IEEE 45th Conference on Local Computer Networks (LCN)*, 2020, pp. 309–320, doi: http://dx.doi.org/10.1109/LCN48667.2020.9314838.

[10] R. E. Kalman, "A New Approach to Linear Filtering and Prediction Problems," in *Transaction of the Asme Journal of Basic*, 1960, online [Available]:http://www.unitedthc.com/DSP/Kalman1960.pdf.

[11] R. Aringhieri, G. Carello, and D. Morale, "Ambulance location through optimization and simulation: the case of milano urban area," in *XXXVIII Annual Conference of the Italian Operations Research Society Optimization and Decision Sciences:1-29*, 2007.

[12] J. Nicholl, J. West, S. Goodacre, and J. Turner, "Tg," *Emergency Medicine Journal*, vol. 24, no. 9, pp. 665–668, 2007, doi:http://dx.doi.org/10.1136/emj.2007.047654.

[13] J. Pell, J. Sirel, A. Marsden, I. Ford, and S. Cobbe, "Effect of Reducing Ambulance Response Times on Deaths from out of Hospital Cardiac Arrest: Cohort Study," *BMJ (Clinical research ed.)*, vol. 322, pp. 1385–8, 07 2001, doi:http://dx.doi.org/10.1136/bmj.322.7299.1385.

[14] A. P. Iannoni, R. Morabito, and C. Saydam, "An optimization approach for ambulance location and the districting of the response segments on highways," *European Journal of Operational Research*, vol. 195, no. 2, pp. 528–542, June 2009, doi: https://ideas.repec.org/a/eee/ejores/v195y2009i2p528-542.html.

[15] M. Poulton, A. Noulas, D. Weston, and G. Roussos, "Modeling Metropolitan-Area Ambulance Mobility Under Blue Light Conditions," *IEEE Access*, vol. 7, pp. 1390–1403, 2019, doi: http://dx.doi.org/10.1109/ACCESS.2018.2886852.

[16] A. Em, M. Sarvi, and S. Bagloee, "Using Kalman filter algorithm for short-term traffic flow prediction in a connected vehicle environment," *Journal of Modern Transportation*, 07 2019, doi:http://dx.doi.org/10.1007/s40534-019-0193-2.

[17] Jiann-Shiou Yang, "Travel time prediction using the gps test vehicle and kalman filtering techniques," in *Proceedings of the 2005, American Control Conference, 2005.*, 2005, pp. 2128–2133 vol. 3, doi:http://dx.doi.org/10.1109/ACC.2005.1470285.

[18] W. Min, L. Yu, P. Chen, M. Zhang, Y. Liu, and J. Wang, "On-Demand Greenwave for Emergency Vehicles in a Time-Varying Road Network With Uncertainties," *IEEE Transactions on Intelligent Transportation Systems*, vol. 21, no. 7, pp. 3056–3068, 2020, doi:http://dx.doi.org/10.1109/TITS.2019.2923802.

[19] K. Nellore and G. Hancke, "A Survey on Urban Traffic Management System Using Wireless Sensor Networks," *Sensors*, vol. 16, p. 157, 01 2016, doi:http://dx.doi.org/10.3390/s16020157.

[20] S. Rimer and G. Hancke, "Actor Coordination Using Info-Gap Decision Theory in Wireless Sensor and Actor Networks," *IJSNet*, vol. 10, pp. 177–191, 10 2011, doi:http://dx.doi.org/10.1504/IJSNET.2011.042769.

[21] S. Joerer, B. Bloessl, M. Segata, C. Sommer, R. L. Cigno, A. Jamalipour, and F. Dressler, "Enabling situation awareness at intersections for ivc congestion control mechanisms," *IEEE Transactions on Mobile Computing*, vol. 15, no. 7, pp. 1674–1685, 2016, doi:http://dx.doi.org/10.1109/TMC.2015.2474370.

[22] H. Nguyen and H. Jeong, "Mobility-Adaptive Beacon Broadcast for Vehicular Cooperative Safety-Critical Applications," *IEEE Transactions on Intelligent Transportation Systems*, vol. 19, no. 6, pp. 1996–2010, 2018, doi:http://dx.doi.org/10.1109/TITS.2017.2775287.

[23] A. Senart, M. Bouroche, and V. Cahill, "Modelling an Emergency Vehicle Early-warning System using Real-time Feedback," *IJIIDS*, vol. 2, pp. 222–239, 01 2008, doi:http://dx.doi.org/10.1504/IJIIDS.2008.018256.

[24] N. Kapileswar, P. V. Santhi, V. K. R. Chenchela, and C. H. V. S. Prasad, "A Fast Information Dissemination System for Emergency Services over Vehicular Ad Hoc Networks," in *2017 International Conference on Energy, Communication, Data Analytics and Soft Computing (ICECDS)*, 2017, pp. 236–241, doi:http://dx.doi.org/10.1109/ICECDS.2017.8389862.

[25] T. Johnson, "Emergency Vehicle Notification System," *U.S. Patent 7,397,356.*, 2005, online [Available]:https://patents.google.com/patent/US7397356.

[26] S. A. Hadiwardoyo, S. Patra, C. T. Calafate, J.-C. Cano, and P. Manzoni, "An intelligent transportation system application for smartphones based on vehicle position advertising and route sharing in vehicular ad-hoc networks," *Journal of Computer Science and Technology*, vol. 33, no. 2, pp. 249–262, 2018, doi:https://doi.org/10.1007/s11390-018-1817-4.

[27] A. Metzner and T. Wickramarathne, "Exploiting Vehicle-to-Vehicle Communications for Enhanced Situational Awareness," in *2019 IEEE Conference on Cognitive and Computational Aspects of Situation Management (CogSIMA)*, 2019, pp. 88–92, doi:http://dx.doi.org/10.1109/COGSIMA.2019.8724309.

[28] Y. Moroi and K. Takami, "A Method of Securing Priority-Use Routes for Emergency Vehicles using Inter-Vehicle and Vehicle-Road Communication," in *2015 7th International Conference on New Technologies, Mobility and Security (NTMS)*, 2015, pp. 1–5, doi:http://dx.doi.org/10.1109/NTMS.2015.7266466.

[29] J. Zhang and K. B. Letaief, "Mobile Edge Intelligence and Computing for the Internet of Vehicles," *Proceedings of the IEEE*, vol. 108, no. 2, pp. 246–261, 2020, doi: https://doi.org/10.1109/JPROC.2019.2947490.

[30] S. A. A. Shah, E. Ahmed, M. Imran, and S. Zeadally, "5G for Vehicular Communications," *IEEE Communications Magazine*, vol. 56, no. 1, pp. 111–117, Jan 2018, doi:http://dx.doi.org/10.1109/MCOM.2018.1700467.

[31] K. Abboud, H. A. Omar, and W. Zhuang, "Interworking of DSRC and Cellular Network Technologies for V2X Communications: A Survey," *IEEE Transactions on Vehicular Technology*, vol. 65, no. 12, pp. 9457–9470, 2016, doi: https://doi.org/10.1109/TVT.2016.2591558.

[32] N. Slamnik-Kriještorac, H. C. Carvalho de Resende, C. Donato, S. Latré, R. Riggio, and J. Marquez-Barja, "Leveraging Mobile Edge Computing to Improve Vehicular Communications," in *2020 IEEE 17th Annual Consumer Communications Networking Conference (CCNC)*, 2020, pp. 1–4, doi:http://dx.doi.org/10.1109/CCNC46108.2020.9045698.

[33] B. Carr, M. Caplan, J. Pryor, and C. Branas, "A meta-analysis of prehospital care times for trauma." *official journal of the National Association of EMS Physicians and the National Association of State EMS Directors*, vol. 7, pp. 198–206, 2006, doi: http://dx.doi.org/10.1080/10903120500541324.

[34] "A review on simulation models applied to emergency medical service operations," *Computers Industrial Engineering*, vol. 66, no. 4, pp. 734–750, 2013, doi: http://dx.doi.org/10.1016/j.cie.2013.09.017.

[35] ETSI, "Intelligent Transport Systems (ITS); Vehicular Communications; Basic Set of Applications; Part 2: Specification of Cooperative Awareness Basic Service," *ETSI ISG ITS, ETSI EN 302 637-2 V1.4.1*, 2019, online [Available]:https://www.etsi.org/deliver/etsi_en/302600_302699/30263702/01.03.02_60/en_30263702v010302p.pdf.

[36] ——, "Multi-Access Edge Computing (MEC); Framework and Reference Architecture," *ETSI ISG MEC, ETSI GS MEC 003 V2.1.1*, 2019, online [Available]: https://www.etsi.org/deliver/etsi_gs/MEC/001_099/003/02.01.01_60/gs_MEC003v020101p.pdf.

[37] ETSI., "Intelligent Transport Systems (ITS); Vehicular Communications; Basic Set of Applications; Part 3: Specification of Decentralized Environment Notification Basic Service," *ETSI ISG ITS, ETSI EN 302 637-3 V1.3.0*, 2018, online [Available]:https://www.etsi.org/deliver/etsi_en/302600_302699/30263703/01.02.01_30/en_30263703v010201v.pdf.

[38] Vanetza, "Vanetza - Open Source ETSI C-ITS protocol suite," 2020, online [Available]:http://http://www.vanetza.org/, Last accessed on 2020-6-1.

[39] J. Marquez-Barja, B. Lannoo, D. Naudts, B. Braem, V. Maglogiannis, C. Donato, S. Mercelis, R. Berkvens, P. Hellinckx, M. Weyn *et al.*, "Smart Highway: ITS-G5 and C2VX based testbed for vehicular communications in real environments enhanced by edge/cloud technologies," in *EuCNC2019, the European Conference on Networks and Communications*, 2019, pp. 1–2, available [Online]:https://biblio.ugent.be/publication/8642435.

[40] U. Klee, T. Gehrig, and J. McDonough, "Kalman filters for time delay of arrival-based source localization," *EURASIP J. Adv. Signal Process. 2006*, vol. 7, 2006, doi:http://dx.doi.org/10.1155/ASP/2006/12378.

[41] A. Shalaby and A. Farhan, "Prediction Model of Bus Arrival and Departure Times Using AVL and APC Data," *Journal of Public Transportation*, vol. 7, 03 2004, doi:http://dx.doi.org/10.5038/2375-0901.7.1.3.

[42] A. Bensky, *Wireless Positioning Technologies and Applications, Second Edition*, 2nd ed. Artech House, 2016.

[43] T. Toledo and D. Zohar, "Modeling duration of lane changes," *Transportation Research Record*, vol. 1999, no. 1, pp. 71–78, 2007, doi: http://dx.doi.org/10.3141/1999-08.

Rreze Halili is a PhD Researcher at the University of Antwerp and IDLab - the core research group of IMEC. She received her Bachelor of Science in Electrical Engineering – Telecommunications and Master of Science in Telecommunications from the University of Prishtina, Faculty of Electrical and Computer Engineering, in 2011 and 2014 respectively. She worked as Teaching Assistant at the University of Prishtina, was an Intern at Robert Bosch Research in Germany, and worked for PECB and Asseco SEE companies. Her research interests involve vehicle localization using wireless communication and satellite technologies, radio wave propagation, path loss models optimization, reliable, and safe wireless cellular communications.

F. Zarrar Yousaf is a Senior Researcher at NEC Laboratories Europe, Germany. He completed his PhD from TU Dortmund, Germany. His current research interest is on NFV/SDN in the context of 5G networks. He is also an active contributor to ETSI ISG NFV standards organization where he holds Rapporteurship for six work-items. He has extensive experience in the design, development, modeling, simulation and prototyping of communication systems and protocols for optimizing overall network performance. He has 04 granted patent and 15 filed patents while his research work has been published in several peer reviewed journals, conferences and book chapters.

Nina Slamnik-Kriještorac is currently a PhD researcher in the field of Applied Engineering Sciences, at the University of Antwerp and the IMEC research center in Belgium. She obtained her Master degree in telecommunications engineering at Faculty of Electrical Engineering, University of Sarajevo, Bosnia and Herzegovina, in July 2016. In the period from 2016 to 2018, she worked as a Teaching Assistant at University of Sarajevo. She authored or co-authored several publications in journals and international conferences. Her current research is mostly based on NFV/SDN-based network architectures with edge computing for vehicular systems, and the management and orchestration of the flexible and programmable next generation end-to-end network resources and services.

Girma M. Yilma is Research Engineer at NEC Laboratories Europe in Heidelberg, Germany. He received his B.Sc. (2010) in Electrical and Computer Engineering from Addis Ababa University, and M.Sc. (2016) in Telecommunications Engineering from University of Trento, Italy. His current research interest is focused around NFV MANO, Orchestration, Cloud Native Network Orchestration, NFV/SDN related technologies in the context of 5G network architecture and operations.

Marco Liebsch is chief researcher at NEC Laboratories Europe GmbH and is working in the area of 5G mobility management, mobile edge computing and content distribution, mobile cloud networking, and software-defined networking. He received his Ph.D. degree from University of Karlsruhe, Germany, in 2007. He worked in different EU research projects and is contributing to standards in the IETF, ETSI and 3GPP. He has a long record of IETF contributions as well as RFC, journal and conference publications.

Rafael Berkvens is a postdoctoral researcher at the University of Antwerp, Belgium. He received his Masters degree in Applied Engineering: Electronics-ICT from the University of Antwerp, in 2012. He received his Ph.D. degree on indoor location information quantification from the same university in 2017, working at the IDLab – imec research group. He currently serves as research and teaching assistant at the University of Antwerp.

Maarten Weyn received his Ph.D. in Computer Science from the University of Antwerp, Belgium. He is a Professor at the University of Antwerp. Maarten is instructor at the LoraWAN Academy on the topic of localization and lecturer in a few courses on Coursera on Embedded IoT systems. His research in the imec-IDlab research group focuses on ultra-low power sensor communication and embedded systems, sub 1-Ghz communication, sensor processing and localization. Most of his projects are in close collaboration with industry. He is the co-founder of the spin-offs Aloxy, CrowdScan and AtSharp, involved in the creation of the spin-offs 1OK and Viloc, director of the Dash7 Alliance, IARIA Fellow and initiator of the Open Source Stack OSS-7.